Rare Metal Materials and Engineering
Volume 50, Issue 2, February 2021
Available online at www.rmme.ac.cn

Science Press

Cite this article as: Rare Metal Materials and Engineering, 2021, 50(2): 0504-0510.

ARTICLE

Dynamic Recrystallization Model of Ultrafine-Grained Pure Zirconium Refined by Compounding

Han Peisheng[1], Ma Weijie[2], Li Yanwei[3], Zhu Xiaoyu[1], Yang Xirong[2], Wang Xiao-gang[1]

[1] Shanxi Provincial Key Laboratory of Metallurgical Device Design Theory and Technology (State Key Laboratory Cultivation Base of Province-Ministry Co-Construct), Taiyuan University of Science and Technology, Taiyuan 030024, China; [2] Metallurgical Engineering School, Xi'an University of Architecture and Technology, Xi'an 710055, China; [3] Jinzhong University, Jinzhong 030619, China

Abstract: An ultrafine-grained (UFG) pure zirconium refined by compounding with grain size of 200~250 nm was subjected to a unidirectional compression test using a Gleeble-3800 thermal simulation tester at the temperatures of 300~450 °C and strain rates of 0.001~0.05 s^{-1}. Experimental results show that the hot process parameters influence the flow stress of the UFG pure zirconium. Experimental data and microstructure analysis reveal that dynamic recrystallization is more likely to occur at higher deformation temperatures and lower strain rates. The critical strain model of UFG pure zirconium was established, and the relationship between the temperature-compensated strain rate factor Z and ε_c (critical strain), σ_c (critical stress), ε_p (peak strain) and σ_p (peak stress) was obtained. The constitutive model of UFG pure zirconium was confirmed based on dynamic recrystalization (DRX) volume fraction and proven to occur at a strain of 0.1 to 0.45.

Key words: ultrafine-grained pure zirconium refined by compounding; thermal compression; microstructure; critical strain; dynamic recrystallization; constitutive model

Zirconium and zirconium alloys exhibit excellent corrosion resistance and processing properties, and have a wide application prospect in the aerospace, medical, chemical and metallurgical industries[1,2]. In the field of plastic microforming where the characteristic size is less than 1 mm in at least two directions, the grain size of conventional coarse-grained pure zirconium is similar to that of micro parts, and the size effect is obvious, which seriously affects the dimensional accuracy and forming quality of micro parts[3]. Ultrafine-grained (UFG) materials with sub-micron and even nanometer grades prepared by severe plastic deformation (SPD) have high strength, high plasticity, and high strain rate superplasticity, thereby improving the surface quality and filling performance of micro-components[4-6]. Various SPD methods can successfully obtain UFG materials, these methods include high-pressure torsion (HPT), equal-channel angular pressing (ECAP), and accumulated roll bonding (ARB). ECAP is currently the most effective method for preparing UFG materials, and it is also the most widely used technology in industries[7-9]. Nevertheless, the shape and size of the UFG crystal materials prepared by ECAP are far from the actual products, and these regard secondary processing methods, such as rolling, forging, and extrusion, can be used to effectively meet product requirements[10]. In this research, UFG pure zirconium with a grain size of 200~250 nm was prepared through ECAP and rotary swaging composite refining process.

The fabricated UFG pure zirconium has the characteristics of high strength and good fatigue performance, but its low plasticity and poor toughness have become key factors that restrict its development, so UFG pure zirconium was thermoplastically deformed to improve the formability of the

Received date: February 08, 2020
Foundation item: National Natural Science Foundation of China (51675362); The Young SAN JIN Scholars' Program
Corresponding author: Wang Xiaogang, Ph. D., Professor, Shanxi Provincial Key Laboratory of Metallurgical Device Design Theory and Technology, Taiyuan University of Science and Technology, Taiyuan 030024, P. R. China, Tel: 0086-351-2776763, E-mail: wxg@tyust.edu.cn

material. Liu et al[11] conducted thermal compression for UFG pure zirconium within a wide range of strain rate and temperature. The UFG pure zirconium underwent significant dynamic recovery (DRV) and dynamic recrystallization (DRX), and the yield strength of UFG pure zirconium was significantly higher than that of coarse-grained pure zirconium. Yang et al[12] conducted research on the high-cycle fatigue of UFG pure zirconium, and the fatigue limit of UFG pure zirconium was 285 MPa after 10^7 cycles, which was 70% higher than that of the coarse-grained pure zirconium. Few reports are available on the DRX model of UFG pure zirconium.

During the thermal processing of UFG pure zirconium, the DRX behavior affects the material's formability by affecting the microstructure. In addition, the DRX behavior is induced when the strain reaches its critical value. Thus, determining the critical strain condition of DRX is the key to judge whether the material has undergone DRX and to measure its difficulty. Moreover, the establishment of the UFG pure zirconium critical strain model and the DRX volume fraction model provides an important basis for material research and process determination.

1 Experiment

In this experiment, we used hot-rolled annealed commercial pure zirconium sheet, and its chemical compositions (wt%) are shown in Table 1. UFG pure zirconium was successfully prepared by ECAP and rotary swaging process. The microstructure is shown in Fig.1. A thermal compression experiment was performed using a Φ4 mm×6 mm cylindrical specimen. The set deformation temperatures were 300, 350, 400, and 450 °C. The strain rates were 0.001, 0.005, 0.01, 0.05 s^{-1}. The maximum deformation was 50%, and the heating rate was 5 °C/s^{-1}. A special graphite sheet was placed between the collet and the end face of the specimen, the microstructure after hot formation was retained by water cooling immediately after deformation. The specimen was split parallel to the compression direction to prepare the metallography of the specimen. The microstructure was observed with a transmission electron microscope (TEM).

Table 1 Chemical compositions of commercial pure zirconium (wt%)

Fe+Cr	C	N	H	O	Zr
≤0.2	≤0.05	≤0.025	≤0.005	≤0.16	Bal.

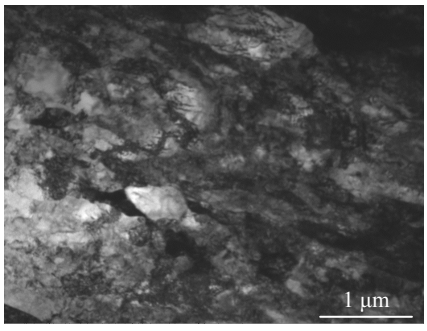

Fig.1 TEM image of UFG pure zirconium

2 Results and Discussion

2.1 Thermal deformation behavior

Fig.2 shows the true stress-true strain curves of UFG pure zirconium under different strain rates and deformation temperatures. As the strain increases, the flow stress rapidly increases and the stress peak appears, and then gradually decreases, thereby showing obvious DRX characteristics. In the initial stage of strain, the flow stress increases rapidly, and presents an obvious work-hardening phenomenon. With increasing the strain, the dislocation density of materials increases, the deformation storage energy increases, and the DRV of materials increases. At this stage, the work hardening rate is significantly higher than the DRV and DRX, and the flow stress increases sharply. After the peak stress, the DRX of the material is enhanced, which can effectively promote the reduction in the dislocation density, resulting in a gradual reduction in the flow stress.

In addition, UFG pure zirconium has obvious sensitivity characteristics of thermal deformation temperature and strain

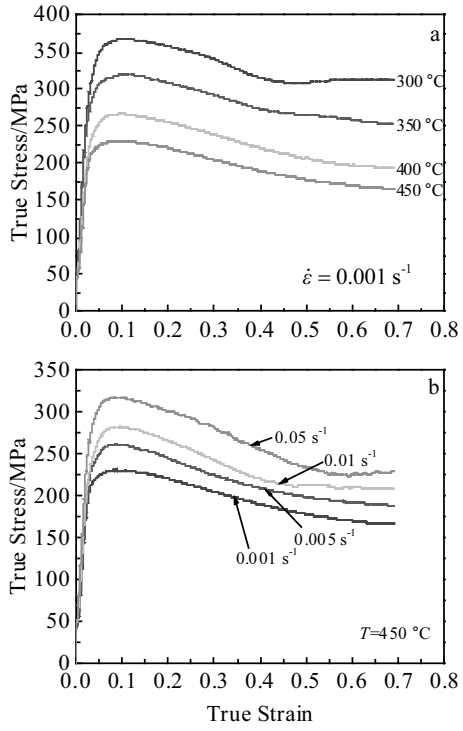

Fig.2 True stress-true strain curves of UFG pure zirconium under various hot processing parameters: (a) $\dot{\varepsilon}$ =0.001 s^{-1} and (b) T=450 °C

rate. With increasing the deformation temperature at the same strain rate, the flow stress of UFG pure zirconium decreases significantly, as shown in Fig.2a. This finding is due to the following: the critical shear stress of the slip system decreases with increasing deformation temperature, the kinetic energy of the metal atoms increases gradually, and point defects such as interstitial atoms and vacancies become more active, resulting in dynamic softening and flow stress reduction. At the same deformation temperature, and with increasing the strain rate, the flow stress of UFG pure zirconium gradually increases, as shown in Fig.2b. With increasing the strain rate, the material becomes more difficult to undergo DRV and DRX, resulting in increased flow stress.

Fig.3 shows the TEM microstructures at different deformation temperatures with a strain rate of 0.001 s^{-1}. When the deformation temperature is 300 °C, the microstructure is filled with higher density dislocations, which accumulate at the grain boundaries, and the material DRV forms a few sub-grains (Fig.3a). When the deformation temperature is 350 °C, the dislocation density in the grain gradually decreases, the grain boundaries gradually become clear, the sub-grain merges to form a large-angle sub-grain with a large size and a sharp interface, and the material changes from DRV to DRX (Fig.3b). As the deformation temperature further increases, the recrystallized grains grow further, the grain boundaries become clearer, and the DRX becomes more obvious (Fig.3c). When the temperature rises to 450 °C (Fig.3d), the grains grow to the maximum and the dislocation density is extremely low. Therefore, significant DRV and DRX occur during the thermal deformation of the UFG pure zirconium.

Fig.4 shows the TEM microstructure after compression at 450 °C and different strain rates. As the strain rate decreases, the dislocation density inside the grain gradually decreases, the grain boundaries gradually become clear, and the recrystallized grains grow significantly. With decreasing the strain rate, the deformation time increases and the recrystallization grains have sufficient time to grow. Overall, UFG pure zirconium is more prone to DRX at higher deformation temperature and lower strain rate.

2.2 Critical strain model of UFG pure zirconium dynamic recrystallization

Critical strain is an important parameter used to calculate DRX constitutive equation. When the strain reaches the critical level, the material will undergo DRX. The critical conditions for DRX can be obtained through numerous microstructure observations or true stress-true strain curves. However the microstructure observation workload is large, the operation is complex, and accurately obtaining the critical conditions for DRX is difficult[13,14]. Ryan et al[15] and Mcqueen et al[16] proposed to determine the critical occurrence conditions through the flow stress curve and the work hardening rate (θ). Therefore, in this work, the critical strain model is determined by the relationship between θ (θ=(dσ/dε)) and σ.

By analyzing the data before the peak point, the θ-σ relation

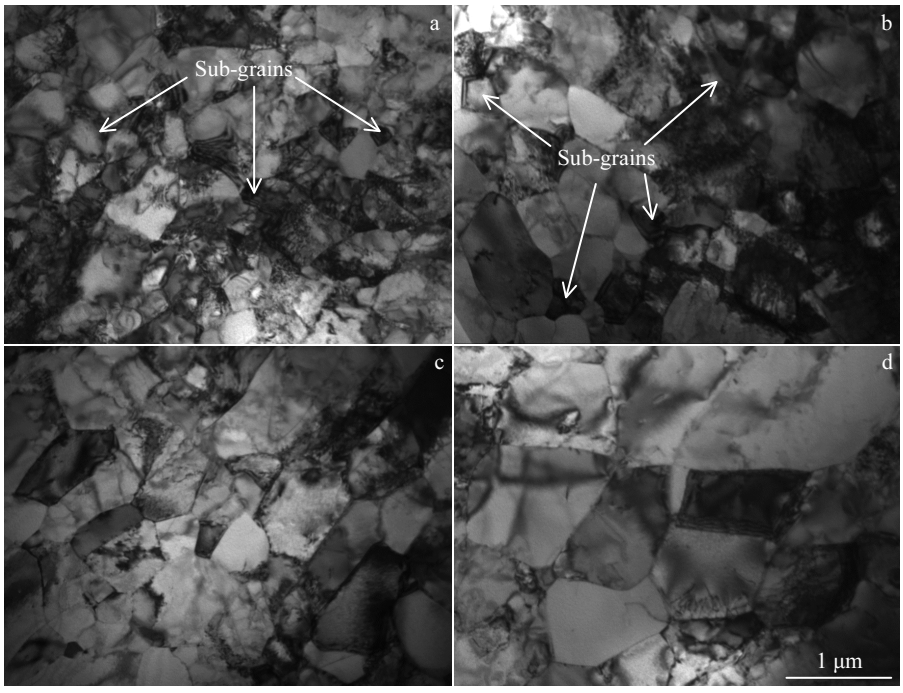

Fig.3 TEM microstructures of UFG pure zirconium at the same strain rate ($\dot{\varepsilon}$ =0.001 s^{-1}) and different deformation temperatures: (a) T=300 °C, (b) T=350 °C, (c) T=400 °C, and (d) T=450 °C

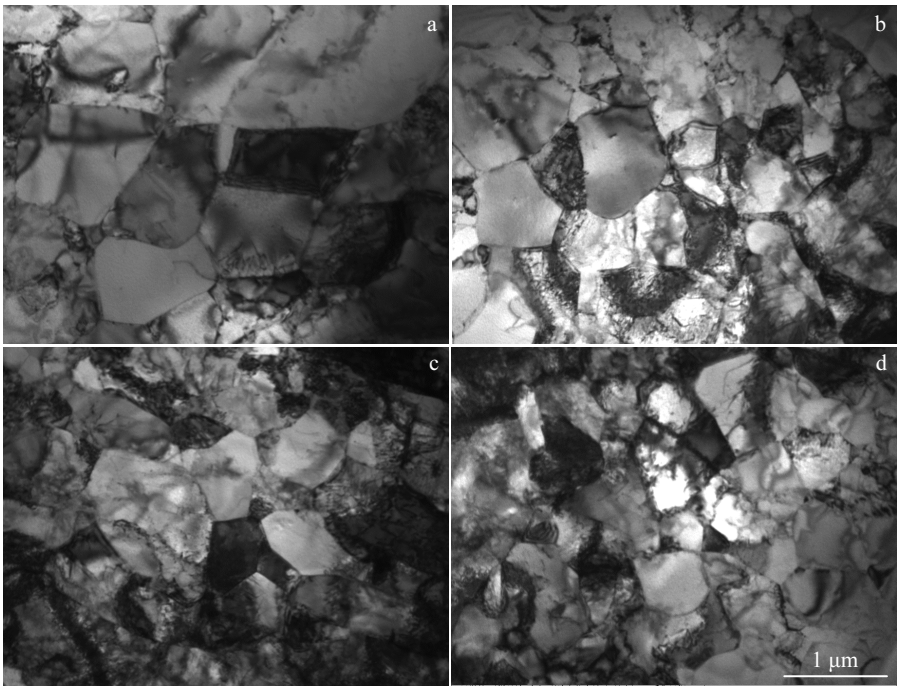

Fig.4 TEM microstructures of UFG pure zirconium at the same deformation temperature (T=450 °C) and different strain rates: (a) $\dot{\varepsilon}$ =0.001 s^{-1}, (b) $\dot{\varepsilon}$ =0.005 s^{-1}, (c) $\dot{\varepsilon}$ =0.01 s^{-1}, and (d) $\dot{\varepsilon}$ =0.05 s^{-1}

is established. Fig.5 shows the θ-σ curves at different deformation temperatures with a strain rate of 0.001 s^{-1}. This curve includes two stages. In the first stage, the dislocation density increases with the applied load and the material DRV occurs, leading to the gradual slowdown in the work hardening rate curve. With increasing the strain at the beginning of the second stage, the material undergoes DRX to weaken the softening phenomenon, and the slope of the curve increases significantly. At this time, the critical stress (σ_c), which is the inflection point of the θ-σ appears. As the strain continues to increase, a stress peak (σ_p) appears, at which the work hardening rate is 0.

This study selects the true stress-true strain curves at T=350 °C and $\dot{\varepsilon}$ =0.001 s^{-1} for specific analysis. Given that the critical strain value is lower than the peak one, the corresponding θ-σ curve is obtained by calculating and analyzing the partial data before the peak stress (Fig.6). The inflection point portion is selected for subsequent analysis.

The selected part is fitted with a fourth-order polynomial, and the inverse of the first order is ascertained to obtain θ-σ curve. As shown in Fig.7, the x-coordinate corresponding to the peak value of the curve is the critical stress value, and can be substituted into the true stress-true strain curve to obtain

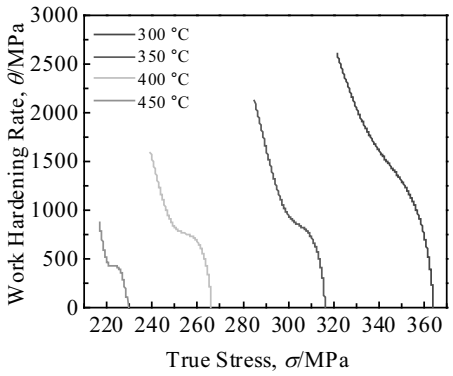

Fig.5 θ-σ curves of UFG pure zirconium at different deformation temperatures with a strain rate of 0.001 s^{-1}

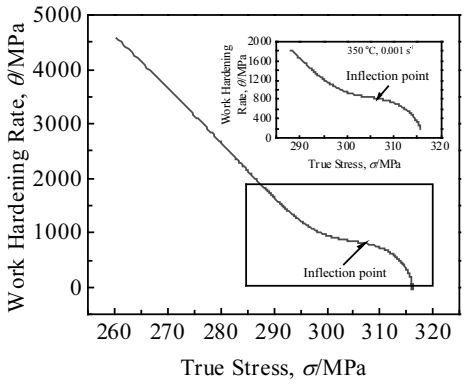

Fig.6 Plot of θ-σ at 350 °C and 0.001 s^{-1}

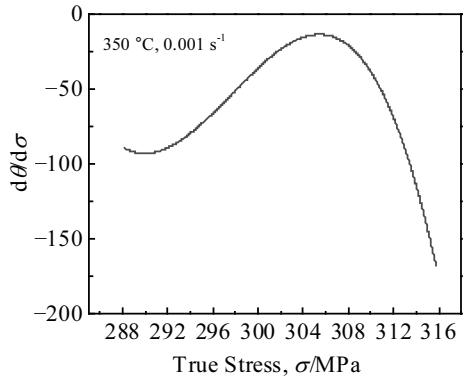

Fig.7 Plot of $d\theta/d\sigma$-σ at 350 °C and 0.001 s^{-1}

the critical strain whose value is 0.050 38 under T=350 °C and $\dot{\varepsilon}$=0.001 s^{-1}.

In general, the critical strain model of the DRX can be expressed by the following relation:

$$\begin{cases}\varepsilon_c = k\varepsilon_p \\ \varepsilon_p = a_1 Z^{a_2}\end{cases} \quad (1)$$

where ε_c is the critical strain of DRX; ε_p is the peak strain, a_1, a_2 are the material parameters; Z is temperature-compensated factor. The DRX critical strain value of UFG pure zirconium under other process parameters can be obtained by the above method. The value of k can be dentified by the linear fitting of ε_c, ε_p values under all process parameters. The result is shown in Fig.8.

According to Fig.8, it can be concluded that:

$$\varepsilon_c=0.54597\varepsilon_p \quad (2)$$

The temperature-compensated factor Z must be introduced to determine the DRX critical strain model containing the Z function[17], and its formula is as follows:

$$Z = \dot{\varepsilon}\exp\left(\frac{Q}{RT}\right) = A[\sinh(\alpha\sigma)]^n \quad (3)$$

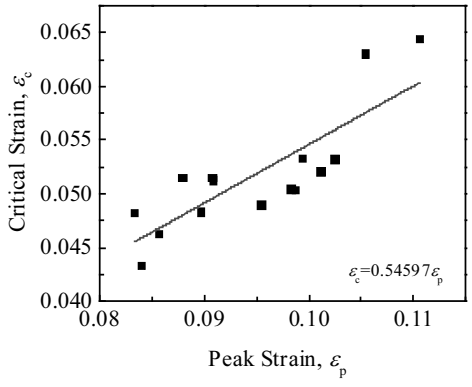

Fig.8 Plot of ε_c-ε_p

where R is the gas constant; T is the absolute temperature; Q is the thermal deformation activation energy of the material; A, α are the material constants; n is the stress index.

Through the transformation of Eq.(3), the activation energy formula of material thermal deformation can be obtained:

$$Q = R\cdot\left[\frac{\partial\ln(\sinh(\alpha\sigma))}{\partial\left(\frac{1}{T}\right)}\right]_{\dot{\varepsilon}}\cdot\left[\frac{\partial\ln\dot{\varepsilon}}{\partial\ln[\sinh(\alpha\sigma_p)]}\right]_T \quad (4)$$

The thermal deformation activation energy of UFG pure zirconium can be finally obtained as Q=105.81 kJ/mol by plotting the relationship curves of $\ln[\sinh(\alpha\sigma_p)]$-$\ln\dot{\varepsilon}$ and $\ln[\sinh(\alpha\sigma_p)]$-$1/T$ (Fig.9).

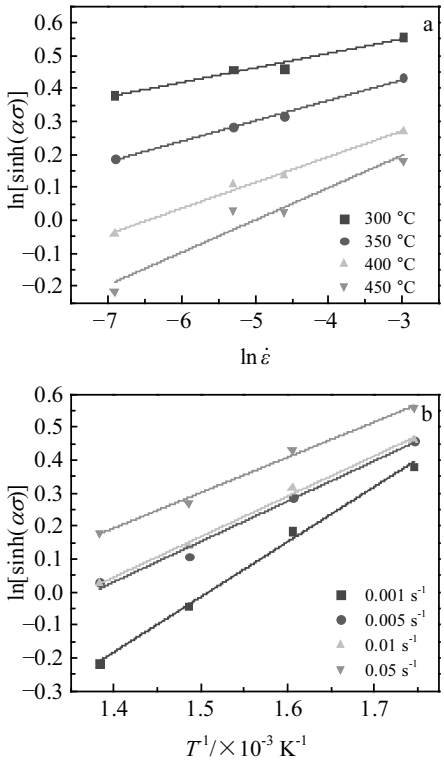

Fig.9 Plots of $\ln[\sinh(\alpha\sigma_p)]$-$\ln\dot{\varepsilon}$ (a) and $\ln[\sinh(\alpha\sigma_p)]$-$1/T$ (b)

The relationship between different thermal processing parameters and temperature compensated factor Z can be obtained [Eq.(5)] by substituting the Q value into Eq.(3):

$$Z = \dot{\varepsilon}\exp\left(\frac{105810}{RT}\right) \quad (5)$$

Fig.10 shows the plot of $\ln\varepsilon_p$-$\ln Z$ under different thermal process parameters. a_1 and a_2 can be determined from the figure as a_1=–2.41076, a_2=–0.00326.

In conclusion, the critical strain model of the DRX of UFG pure zirconium can be determined as

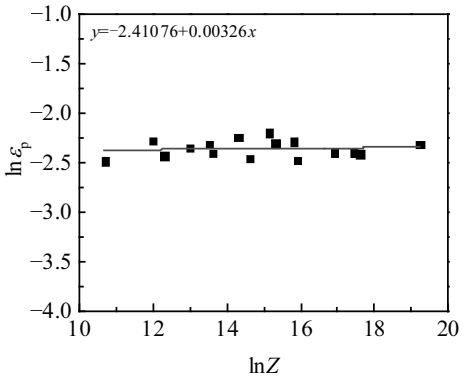

Fig.10 Plot of lnε_p-ln$Z$

$$\begin{cases}\varepsilon_c = 0.54597\varepsilon_p \\ \varepsilon_p = -2.41076Z^{0.00326}\end{cases} \quad (6)$$

2.3 Constitutive model of UFG pure zirconium based on DRX volume fraction

During thermal deformation, DRX occurs when critical strain is reached, and the degree of DRX can be expressed by the DRX volume fraction. The relationship between the DRX volume fraction X_{DRX} and σ based on the true stress-true strain curve is as follows:

$$X_{DRX} = \frac{\sigma - \sigma_p}{\sigma_{ss} - \sigma_p} \quad (7)$$

where X_{DRX} is the DRX volume fraction; σ is the true stress that occurred during DRX; σ_{ss} is the steady state stress that occurred during DRX; σ_p is the peak stress; σ_{ss}, σ_p can be obtained directly from the true stress-true strain curve.

Fig.11 shows the X_{DRX}-ture strain relation curves of UFG pure zirconium at deformation temperature of 300 °C and different strain rates.

The relationship between X_{DRX} and the true strain is as follows[18,19]:

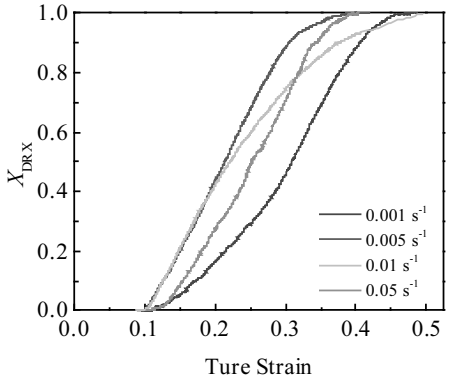

Fig.11 X_{DRX}-ture strain curves of UFG pure zirconium at 300 °C and different strain rates

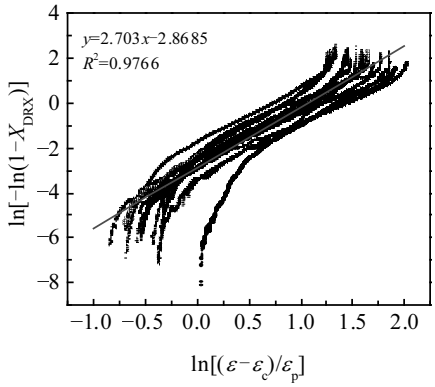

Fig.12 Plot of ln[–ln(1–X_{DRX})]-ln[(ε–ε_c)/ε_p]

$$X_{DRX} = 1 - \exp\left[-k_1\left(\frac{\varepsilon - \varepsilon_c}{\varepsilon_p}\right)^{k_2}\right] \quad (8)$$

where X_{DRX} represents the DRX volume fraction; ε_c is the critical strain; ε_p is the peak strain; k_1, k_2 are the material parameters. Taking the natural logarithms on both sides of the formula yields the following equation:

$$\ln[-\ln(1 - X_{DRX})] = \ln k_1 + k_2 \ln\left(\frac{\varepsilon - \varepsilon_c}{\varepsilon_p}\right) \quad (9)$$

The X_{DRX}, ε_c and ε_p values obtained under different process parameters are substituted into Eq.(9) to obtain the ln[–ln(1–X_{DRX})]-ln[(ε–ε_c)/ε_p] relation curve (Fig.12).

The constitutive model of DRX of UFG pure zirconium can be determined as:

$$X_{DRX} = 1 - \exp\left[-0.0568\left(\frac{\varepsilon - \varepsilon_c}{\varepsilon_p}\right)^{2.703}\right] \quad (10)$$

3 Conclusions

1) Under the same deformation amount, UFG pure zirconium with a grain size of 200~250 nm exhibits obvious sensitive characteristics of thermal deformation temperature and strain rate. With the increase of deformation, the flow stress rapidly increases and the stress peak appears, and then gradually decreases, showing an obvious dynamic recrystallization characteristic.

2) According to the analysis of the true stress-true strain curves of UFG pure zirconium, the activation energy Q= 105.81 kJ/mol. By introducing temperature-compensated factor Z, a critical strain model of UFG pure zirconium is established:

$$\begin{cases}\varepsilon_c = 0.54597\varepsilon_p \\ \varepsilon_p = -2.41076Z^{0.00326}\end{cases}.$$

3) The DRX behavior of UFG pure zirconium occurs at strains of 0.1~0.45, and the constitutive model of UFG pure zirconium based on DRX volume fraction is confirmed:

$$X_{\mathrm{DRX}}=1-\exp\left[-0.0568\left(\frac{\varepsilon-\varepsilon_{\mathrm{c}}}{\varepsilon_{\mathrm{p}}}\right)^{2.703}\right]$$

References

1 Li Xianjun. *Titanium Industry Progress*[J], 2011, 28(1): 38 (in Chinese)

2 Li Peizhi, Tian Zhenye, Shi Yufeng. *Rare Metal Materials and Engineering*[J], 1984(1): 62 (in Chinese)

3 Raulea L V, Goijaerts A M, Govaert L E *et al*. *Journal of Materials Processing Technology*[J], 2001, 115(1): 44

4 Vollertsen F, Biermann D, Hansen H N et al. *CIRP Annals-Manufacturing Technology*[J], 2009, 58(2): 566

5 Xu J, Zhu X C, Shi L *et al*. *Advanced Engineering Materials*[J], 2015, 17(7): 1022

6 Engel U, Eckstein R. *Journal of Materials Processing Technology*[J], 2002, 125-126: 35

7 An B, Li Z, Diao X *et al*. *Materials Science and Engineering C* [J], 2016, 67: 34

8 Hajizadeh K, Eghbali B, Topolski K *et al*. *Materials Chemistry and Physics*[J], 2014, 143(3): 1032

9 Rodriguez-Calvillo P, Cabrera J M. *Materials Science and Engineering A*[J], 2015, 625: 311

10 Gunderov D V, Polyakov A V, Semenova I P *et al*. *Materials Science and Engineering A*[J], 2013, 562: 128

11 Liu Xiaoyan, Yang Cheng, Luo Lei *et al*. *Chinese Journal of Rare Metals*[J], 2019, 38(5): 500 (in Chinese)

12 Yang Xirong, Liu Feng, Luo Lei *et al*. *Rare Metal Materals and Engineering*[J], 2019, 48(8): 2609 (in Chinese)

13 Galindo-Nava E I, Rae C M F. *Materials Science and Engineering A*[J], 2015, 636: 434

14 Galindo-Nava E I, Rivera-Díaz-del-Castillo P E J. *Scripta Materialia*[J], 2014, 72-73: 1

15 Ryan N D, Mcqueen H J. *Canadian Metallurgical Quarterly*[J], 1990, 29(2): 147

16 Mcqueen H J, Ryan N D. *Materials Science & Engineering A* (*Structural Materials: Properties, Microstructure and Processing*) [J], 2002, 322(1-2): 43

17 Shukla A K, Narayana Murty S V S, Sharma S C *et al*. *Materials & Design*[J], 2015, 75: 57

18 Lin Y C, Chen X M, Wen D X *et al*. *Computational Materials Science*[J], 2014, 83: 282

19 Lv B J, Peng J, Shi D W *et al*. *Materials Science and Engineering A* (*Structural Materials: Properties, Microstructure and Processing*)[J], 2013, 560: 727

复合细化超细晶纯锆动态再结晶模型研究

韩培盛[1]，马炜杰[2]，李艳威[3]，朱晓宇[1]，杨西荣[2]，王效岗[1]

(1. 太原科技大学 山西省冶金设备设计理论与技术省部共建国家重点实验室培育基地，山西 太原 030024)

(2. 西安建筑科技大学 冶金工程学院，陕西 西安 710055)

(3. 晋中学院，山西 晋中 030619)

摘　要：采用 Gleeble-3800 热模拟试验机对晶粒尺寸为 200~250 nm 的复合细化超细晶纯锆在变形温度为 300~450 ℃，应变速率为 0.001~0.05 s^{-1} 的范围内进行单向热压缩实验。结果表明：热加工参数对超细晶纯锆流动应力影响很大。通过实验数据以及显微组织分析可知，在较高的变形温度和较低的应变速率下更容易发生动态再结晶；构建了超细晶纯锆的临界应变模型，得出其温度补偿应变速率因子 Z 与 ε_{c} (临界应变)，σ_{c} (临界应力)，ε_{p} (峰值应变)和 σ_{p} (峰值应力)间的关系；建立了超细晶纯锆动态再结晶体积分数模型，可以看出其动态再结晶发生的阶段为应变 0.1~0.45。

关键词：复合细化超细晶纯锆；热压缩；微观组织；临界应变；动态再结晶；本构模型

作者简介：韩培盛，男，1994 年生，博士生，太原科技大学山西省冶金设备设计理论与技术省部共建国家重点实验室培育基地，山西太原 030024，电话：0351-2776763，E-mail: 15234016403@163.com